

Measurement errors and scaling relations in astrophysics: a review

S. Andreon,^{1,*} M. A. Hurn,²

¹INAF–Osservatorio Astronomico di Brera, Milano, Italy

²University of Bath, Department of Mathematical Sciences, Bath, UK

October 24, 2012

Abstract

This review article considers some of the most common methods used in astronomy for regressing one quantity against another in order to estimate the model parameters or to predict an observationally expensive quantity using trends between object values. These methods have to tackle some of the awkward features prevalent in astronomical data, namely heteroscedastic (point-dependent) errors, intrinsic scatter, non-ignorable data collection and selection effects, data structure and non-uniform population (often called Malmquist bias), non-Gaussian data, outliers and mixtures of regressions. We outline how least square fits, weighted least squares methods, Maximum Likelihood, survival analysis, and Bayesian methods have been applied in the astrophysics literature when one or more of these features is present. In particular we concentrate on errors-in-variables regression and we advocate Bayesian techniques.

Keywords: Astrophysics; Bayesian statistics; Errors-in-variables; Measurement errors; Regression; Scaling relations.

1 Introduction

In astrophysics, the term “scaling relation” is taken to mean a relationship between different physical values of astronomical objects such as, stars, galaxies, galaxy clusters and black holes. In more statistical terms, the term indicates a relationship between two variables, Equation (1), along with an associated measure of variability associated with that relationship. Some well-known examples are the Tully-Fisher relation (between galaxy luminosity and circular velocity), the Faber-Jackson relation (between galaxy luminosity and velocity dispersion), the fundamental plane (between galaxy brightness and velocity dispersion and size), the Magorrian relation (between the mass of a black hole and the bulge mass). These relationships are of considerable interest because from their existence and from their parameters we can elaborate or test theories about the object formation and evolution. At a high level, we can make inference from these relationships about the Universe’s birth and fate, or the mysterious dark energy, etc. For example, the Cepheid period-luminosity scaling informs us about the physics regulating these objects, and, at the same time, in the 1930’s demonstrated that the Universe is larger than our own Galaxy, that nebulae are outside our own Galaxy and that the Universe is formed by galaxy-islands ([1]).

Unfortunately it is rarely possible to measure values completely without error. Errors may be deterministic (e.g. rounding to the nearest integer), stochastic or both. In this article, we concentrate on the problem of stochastic noise and we review the interesting statistical questions which arise and the associated methodology currently in the literature. We begin with a simple example to illustrate some of the points which may occur. Suppose we are given N pairs of observations, x_i^{obs} and corresponding y_i^{obs} for data points $i = 1, \dots, N$. The x_i^{obs} are observations on the true values x_i , while the y_i^{obs} are observations on the true values y_i . It would be common in this field to plot y^{obs} against x^{obs} to try to learn something either about the

*stefano.andreon@brera.inaf.it

objects under study, or, via them, about a bigger objective, such as the geometry of our Universe. Expressed more formally, estimating the relationship between the true values x_i and y_i is of interest

$$y_i = f(x_i, \theta) \tag{1}$$

where θ represents any parameters of the relationship. In the simplest case, the function f could be a linear relationship, with θ representing the slope a and intercept b :

$$y_i = ax_i + b. \tag{2}$$

If the $\{x_i\}$ are actually observed without error (in other words, $x_i^{obs} = x_i$) and the $\{y_i\}$ are each corrupted by an additive Normal, or Gaussian, error with constant variance, $y_i^{obs} = y_i + \epsilon_i$ where $\epsilon_i \sim N(0, \sigma^2)$, for $i = 1, \dots, N$, then this problem is the familiar linear regression (the notation \sim reads “is distributed as” throughout). Sadly for astronomers, but perhaps happily for statisticians, things are rarely this simple.

In this article, we will begin in Section 2 by discussing some of the reasons why astronomers are interested in regression. Section 3 describes some of the complicating features that are common in astronomical data. In light of these features, we review the current state of the literature, mostly astronomical, in Section 4. Section 5 will compare the performances of some of these regression methods on simple data. This review only addresses scaling relations in astronomy between physical values, given the breadth of the applications and the volume of statistical methodology involved we do not attempt to tackle spatial or temporal models.

2 Why astronomers regress

There are a number of different reasons why astronomers may have an interest in regressing one quantity against another. These include

- *Parameter estimation.* It may be that the parameters of the relationship between x and y are themselves the primary interest, as in the slope of the cluster of galaxies $L_X - T$ (X-ray luminosity vs Temperature) scaling relation. Usually, we are interested in both the parameter estimates and their estimated uncertainty. When the relationship is important because of what it implies for a higher-level question (for example, Universe geometry), then it is particularly important to carry forward the parameter uncertainty into any higher-level inference. We emphasise that, most of times, we are interested in the relation between the true values x and y , rather than between the observed values x^{obs} and y^{obs} .
- *Prediction.* It may be the case that there is a considerable difference in either the difficulty or the cost of measuring x^{obs} and y^{obs} . Provided there is a trend between the two values and not too much scatter, it might then be desirable to predict the expensive values of y (say) using the cheaper measurements of x , x^{obs} . Two examples from astronomy are the use of colours to predict redshift (see [2] for example), and the use of one of the many cheaper values to predict mass (for example richness [3]). The emphasis here is on assessing the uncertainty associated with the predicted values of y .
- *Model selection.* It may be that the form of the relationship between x and y is of primary interest, that is determining the particular $f(x, \theta)$ in Equation (1), with all this implies for the astrophysics. The important topic of more formal model choice is outside the scope of this review, see instead for example [4] and [5].

To illustrate how the goals of an analysis can alter what may be considered a good model, Figure 1 shows a set of 500 points drawn from a bivariate Gaussian where marginally both x and y are standard Gaussians with mean 0 and variance 1 and x and y have correlation 1/2. What is the “best” line explaining the relationship between x and y here? If we are trying to summarise the relationship itself, then the blue $y = x$ line shown

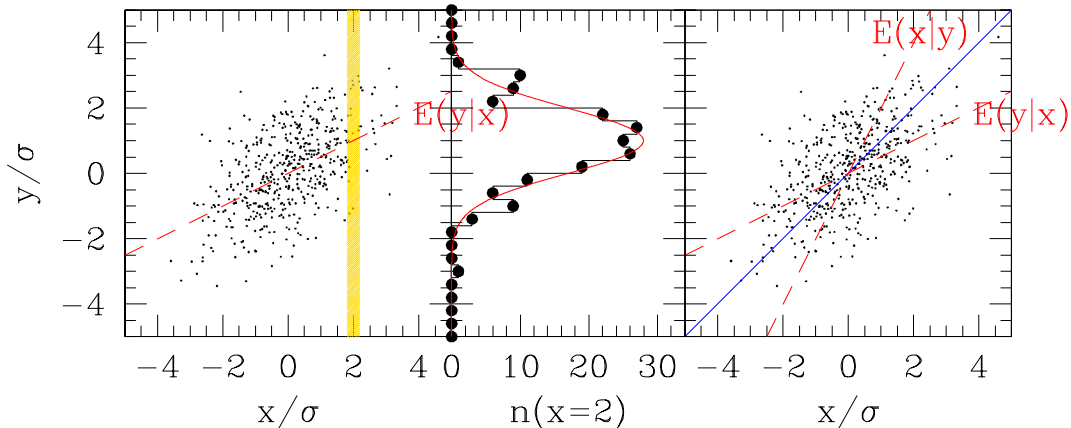


Figure 1: Left panel: 500 points drawn from a bivariate Gaussian overlaid by the line showing the expected value of y given x ; the yellow band covers those y for which x is close to 2. Central panel: Distribution of the y values for x values in a narrow band of x centred on 2, as shaded in the left panel. Right panel: as the left panel, but adding the lines giving the expected x values at a given y , and the $x = y$ line.

on the right hand panel seems reasonable. But is this also good if instead we were trying to predict a new value of y given a value of x ? Superimposed in red on the left hand panel of Figure 1 is the line giving the theoretical conditional expectation of y given x (known theoretically for this bivariate Gaussian to be $y = x/2$). Why might this be a better line for the purposes of prediction? Consider a small range of x values close to 2 indicated in yellow. The middle panel indicates the corresponding y values of the points captured in this way (overlaid on the theoretical distribution of $y|x = 2$, where the symbol $|$ will be used throughout to indicate “conditional on”). The average of the y values falling in the shaded area is closer to the value predicted by the red line (a value of 1 in this case) than to the value predicted by the blue, $y = x$, line (2 in this case). Although this line then is good for prediction, it perhaps seems too shallow with respect to the overall trend identified by the points, which is better captured by the $x = y$ blue line. [6] provides a nice discussion of these issues, and we offer a further example in Section 5.

Figure 1, taken from [3], illustrates one further point, namely the asymmetry of regression. If, rather than predicting y from x , one wishes to do the reverse and predict x given y , then the line defined by the conditional expectation of x given y may be useful. Shown in red in the third panel, this line is different again from the previous two. In this example, the symmetry of the marginal distributions of x and y is reflected in the symmetry of the two red lines. However there is an underlying conceptual difference between the two predictions given that we regard one variable as a predictor and the other as a response. In a slightly more complex setting than this, [7] emphasises that while this is known to many astronomers, not all appreciate the consequences of the difference between the direct and inverse fit in the context of the Magorrian relation (where $x = L$ is the galaxy luminosity and $y = M_{\bullet}$ is the black hole mass). Astronomers may often find themselves in situations where a symmetric treatment of variables would be more natural than a “predictor-response” approach.

3 Common features of astronomical data

3.1 Heteroscedastic error structure

Much standard statistical theory deals with the situation where all observations are made with the same accuracy in the sense that the sizes (variances) of the errors are assumed equal, say σ_y^2 for all the observations,

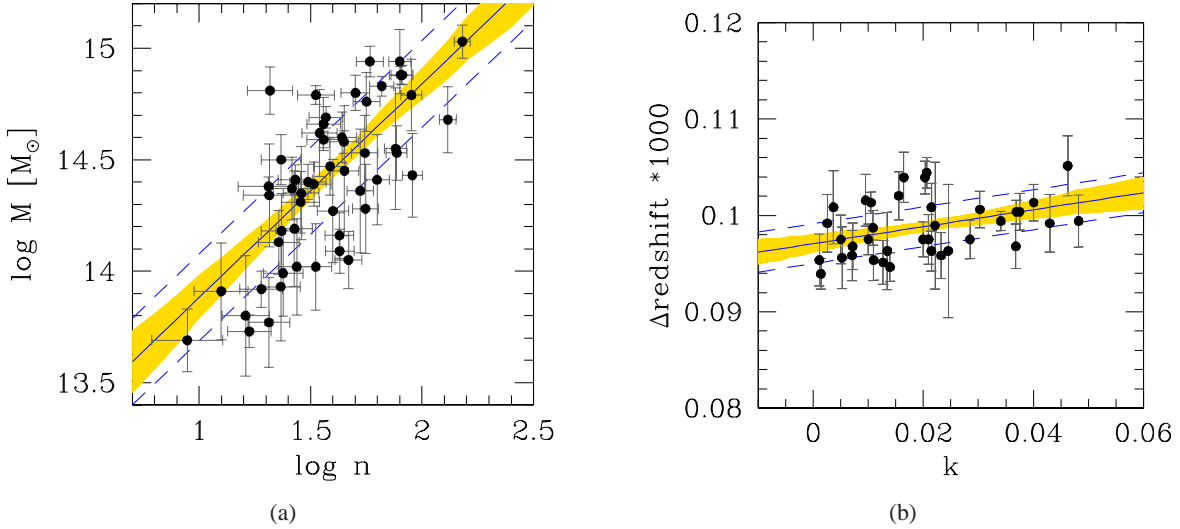


Figure 2: (a) Mass (M) vs Richness (n) (taken from [3]); these data represent galaxy clusters, each point corresponding to a different cluster. Mass is one of holy grails in astronomy but it is observationally expensive or even impossible, to measure, whilst at the same time being needed in many studies because most properties depend on mass. The easily observed quantity richness (n) could in this respect be useful to predict mass. (b) Wavelength shift ($1000 * (\Delta\lambda/\lambda - 3.0248)$), vs sensitivity (k) to physical constant (data taken from [8]); the points correspond to different measurements on a single object, the quasar 3C295. One of the pressing questions in astronomy and physics is whether physical constants are indeed constant or take different values at different locations in the Universe or at different times. The slope of the regression, if different from zero, implies that (a specific combination of) physical constants are not taking a unique value everywhere in the Universe, being different between Earth laboratories and the very distant Universe probed by the plotted experimental points. In both panels the solid line marks the fitted regression, taking into account the intrinsic scatter as well as the measurement noise, while the dashed lines show this plus or minus the estimated intrinsic scatter σ_{scat} derived from the Bayesian analysis in [3]. Error bars on the data points represent the scale (size) of measurement errors, indicating one standard deviation. Distances between the data and the regression are due to both measurement error and intrinsic scatter. (The shaded regions mark 68% highest posterior credible intervals for the regression.)

e.g

$$y_i^{obs} = y_i + \epsilon_i \text{ where } \epsilon_i \sim N(0, \sigma_y^2), i = 1, \dots, N. \quad (3)$$

Such a simplifying assumption is unlikely to be valid in many astronomical studies where a heteroscedastic error structure may have to be adopted, e.g replacing Equation (3) by

$$y_i^{obs} = y_i + \epsilon_i \text{ where } \epsilon_i \sim N(0, \sigma_{y,i}^2), i = 1, \dots, N. \quad (4)$$

The notation $\sigma_{y,i}^2$ is adopted here for later compatibility with situations where the related variable x_i^{obs} also exhibits heteroscedastic error. There are a number of reasons why Equation (4) may be more appropriate, sometimes because the N objects may not be observed under identical conditions, for example, under variable atmospheric conditions, sometimes because of object related differences, for example other values of the object such as luminosity, colour, size, etc. As an additional complication, it is possible for the error structure on the i^{th} object, x_i and y_i , to be correlated; [9] discusses the example of the Tully-Fisher relation where an inclinational correction applied to a galaxy affects both its luminosity and velocity errors.

3.2 Intrinsic scatter

Equations (1) and (2) assume that the relationship between the N objects' values $\{x_i\}$ and $\{y_i\}$ is deterministic, albeit unknown. In many cases, this clean relationship is not representative and there is also an intrinsic scatter (a stochastic variability) to consider. This extra layer of variability is distinct from the (possibly heteroscedastic) measurement noise, indicating instead that the objects under study are examples drawn from a population with a spread of values. Extending the model in Equation (2) to include intrinsic scatter, the full set of equations becomes

$$\begin{aligned} x_i^{obs} &= x_i + \epsilon_{x,i} \text{ where } \epsilon_{x,i} \sim N(0, \sigma_{x,i}^2) \\ y_i^{obs} &= y_i + \epsilon_{y,i} \text{ where } \epsilon_{y,i} \sim N(0, \sigma_{y,i}^2) \\ y_i &\sim N(ax_i + b, \sigma_{scat}^2). \end{aligned} \quad (5)$$

At this point a formal distinction between the two types of measurement error found in the literature should be noted since we have made a choice by specifying Equation (5): the situation above where a distributional assumption is made about the observed data given the true values is called the ‘‘classical measurement error’’ model; if the reverse is true and the distributional assumptions are made about the true values given the observed ones, then the model is known as ‘‘Berkson error’’ ([10], Chapter 1). We will work throughout with the classical model, because the latter is usually available in physics and astronomy and called calibration when dealing with instruments: one injects x in the apparatus and measure the distribution of observed data, $p(x^{obs}|x)$.

Two examples where intrinsic scatter is relevant are shown in Figure 2. The left panel of Figure 2 shows a mass vs richness scaling where the variability between objects is greater than that simply due to measurement errors and is more likely due to differences of the physics on the objects under study ([3]). In other cases, the scatter may be due to unaccounted systematic effects. The right hand plot reports the ratio between the wavelength of several spectral lines compared to the wavelength measured in laboratory, $(\lambda_{obs} - \lambda_{lab})/\lambda_{lab} = \Delta\lambda/\lambda$ against the parameter k , measuring the sensitivity of the considered spectral lines to the physical constant k ([8]). The intrinsic spread visible is due to a source of error still not identified, because all these measurements pertain to a single object and so there is no ‘‘population’’ variability effect.

3.3 Non-ignorable data collection and selection effects

In an ideal world, the sample we have is randomly selected from the population we wish to study, and so any inference we draw about the sample applies to the population; in other words, we can ignore the way in

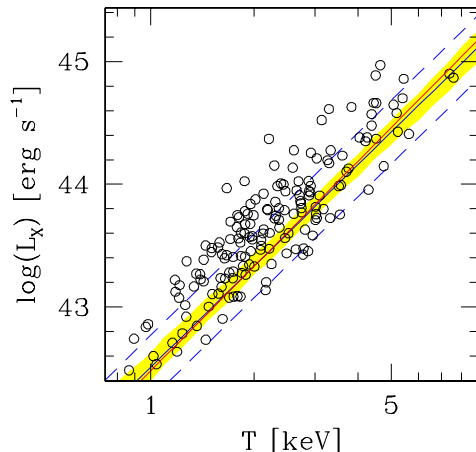


Figure 3: A simulation (from [11]) built around a true $L_X - T$ data set and selection function (from [12]), illustrating how the observed data may be unrepresentative compared to the underlying scaling relation due to selection effects. The solid blue line shows the true relationship but due to the selection effects, most points lie above the line.

which the data were collected. Unfortunately, data collection is very often non-ignorable. As an example, in [7] studying black hole masses, galaxies at high redshift are selected by their nuclear activity while galaxies at low redshift are selected by luminosity or velocity dispersion. But as that paper points out, these two subpopulations are not homogeneous because of the spread in luminosity at any given black hole mass and therefore the effect of the selection criteria may be different for the two. In this particular case, ignoring this selection effect difference leads to biased estimation. At this point, it may be worth giving a formal definition of bias. Statisticians define the “bias” of estimators to be the difference between the expected value of the estimators and the true value of the parameters; however the term “biased” is also widely used to refer to the non-representative nature of a sample (effectively the source of the statistical bias).

Selection effects can arise in a number of forms: a) Object values may be partially missing in a non-random way although the object is in the catalogue. This means we can say something about the missing object, e.g. its position in the sky, but we are lacking a measurement of the quantity of interest; b) The object itself is missing from the catalogue (not at random), and often we can say little or nothing about what is missing, including any idea of how many objects are missing; c) In an extension of the above scenarios, objects can be missing with a probability different from zero or one, for example objects above/below some threshold enter/exit the sample with some probability p , where p is usually a smooth function of the object’s parameters. This case is illustrated in Figure 3, taken from [11]. At all temperatures T , clusters brighter than average are easier to detect (simply because they are brighter) and therefore they are over-represented in most samples, while those fainter than the average are underrepresented. Therefore, at a given T the mean L_X of clusters in the sample is higher than the average L_X of the population at the same T . The selection is stochastic: it is possible to miss an object above the threshold and yet still to record some objects below the threshold. This effect is self-evident and is called the “bias” of the X-ray selected clusters in [13], and the “halo model” in [14], but its consequences are not always fully appreciated, as emphasised in [13]. We will return to these ideas in Sections 4.6 and 6.

Since collecting samples with known (and thus hopefully correctable) selection functions is observationally hard, the issue of selection effects and modelling data collection is often deferred until a selection effect becomes apparent in the data themselves. Often, astronomers are forced to study the property of the population entering in the sample (SDSS or Galax galaxies, PG QSO, EROs), instead of the property of the population sample, because either the selection function is poorly known or it is so severe that it is

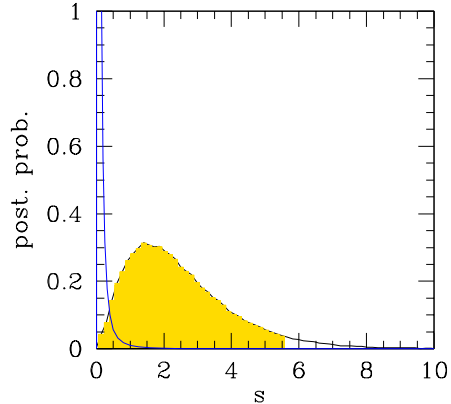


Figure 4: Posterior distribution (black curve) of the source flux, having observed four photons and knowing that source number counts have an Euclidean distribution, that is their probability distributions follow a power law (shown by the blue curve). The highest posterior 95% interval of the source flux is shaded in yellow (adapted from [18]).

impossible to make inference about the wider population.

3.4 Data structure and non-uniform populations

Even when the data collection does not contain selection problems, neglecting the population structure can induce estimation biases: [15] and [16] reminded the astronomical community that even symmetric errors (for example, Gaussian likelihoods) have an effect, later called the Eddington or Malmquist bias.

Figure 4 illustrates the problem using an example from the X-Bootes survey ([17]) of X-ray sources performed with the Chandra Space Telescope. The observation here s^{obs} is a count measurement on the underlying flux, s . As such, we can assume that given the underlying flux s , the data point s^{obs} is distributed as a Poisson random variable, $s^{obs} \sim \mathcal{P}(s)$. However it is also known from previous accurate observations, that the probability distribution of s (known as the number counts by astronomers) is a power law with slope -2.5 (in the standard astronomical units this slope is referred to as the Euclidean slope). This distribution is illustrated in blue on Figure 4 showing that small values of s are more likely than large ones. Therefore, a source with s^{obs} is more likely overall to be a fainter source with an overestimated flux than a stronger one which has been underestimated. This effect has nothing to do with the asymmetric Poisson distribution, it would still be there if a Gaussian noise structure were assumed. Using Bayesian methodology (as described in Section 6), Figure 4 shows the number counts and the posterior distribution of the object flux for a source with four observed photons, $s^{obs} = 4$, typical of the X-Boote survey. The posterior distribution has its mode at $s = 1.5$ and mean at $s = 2.5$, in agreement with astronomical experience that the true flux, s , of a source is likely to be lower than the observed value, s^{obs} .

Whether or not a Bayesian approach is preferred, most astronomers would agree that some form of bias correction is often needed. Such bias is widespread in astronomy, applying not only to fluxes, but almost to all quantities which have an abundance gradient, such as galaxy cluster richnesses (number of galaxies) or masses, parallaxes (i.e. the small angular displacement of stars due to the Earth’s orbit around the Sun), velocity dispersions (how fast galaxies move inside clusters of galaxies or how fast stars move in globular clusters). This has an obvious impact on the determination of regression parameters of scaling relations using these quantities, but its consequences are not always fully appreciated, as emphasised in [3].

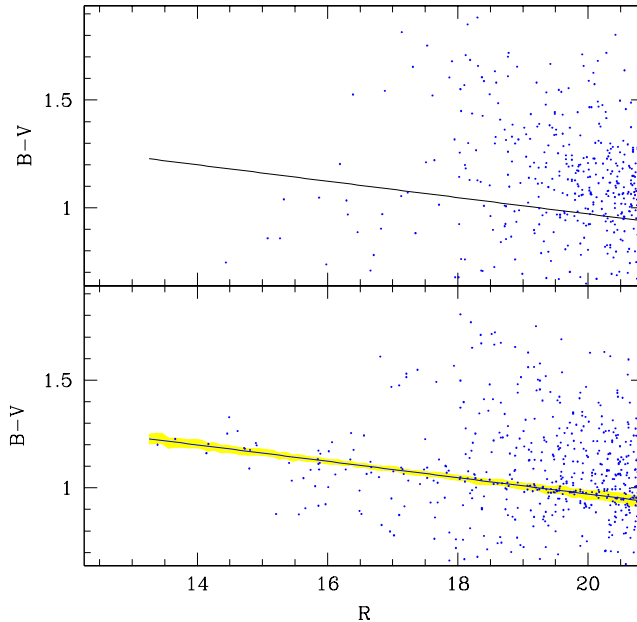


Figure 5: The $B - V$ colour vs R magnitude relation of galaxies (from [21]), where $B - V$, short for blue minus visual magnitudes, is a colour index used in classification and the R magnitude is -2.5 times the base 10 log of the source flux plus a constant. The spread in colour around the mean regression, called in astronomy the colour-magnitude relation, is a measure of heterogeneity in the star-formation histories of red cluster galaxies; the larger the spread, the more variable their star formation histories are. *Top panel:* diagram for galaxies in a random line of sight, showing a realization of contaminating galaxies. *Bottom panel:* diagram for interesting galaxies belonging to the cluster Abell 1185, plus contaminating galaxies, i.e. galaxies in the cluster line of sight but unrelated to the cluster. Which individual point is interesting rather than contaminating is initially unknown. As a result interesting galaxies form a regression heavily contaminated by outliers (there are 4 contaminants per interesting point). The solid line is the mean colour-magnitude relation of interesting galaxies fitted from the lower plot and overlaid on both plots, the narrow yellow area marks the 68% highest posterior interval (lower plot only).

3.5 Non Gaussian data, outliers and other complications

Astronomical data, like all data, can be affected by a number of other problems which negatively affect a regression analysis. For start, it is quite common for the error structure to be other than Gaussian, particularly in situations where small numbers of counts are recorded (even for large numbers of counts, a Gaussian approximation may be not acceptable, see [19]). For example, in the left-hand panel of Figure 2 the x-axis plots the log of a quantity which is (close to being) Poisson distributed.

Another very common problem is that of outliers and contaminated samples; as soon as one collects a sizable sample, it is quite possible to also collect data for objects having little to do with the population of interest. When these objects fall far away from the model suggested by the regression, they are called outliers and some sort of outlier identification and removal may be needed, although removal may only be essential in cases where the outlier is influential (see [20], Chapters 1 to 5, for more information on assessing outliers as well as other important diagnostic aspects of regression modelling).

There can be situations where the level of contamination by data points not following the hypothesised regression model makes it hard to identify the true population under study. Figure 5 gives an example of such a situation where the sample of interest is overwhelmed by other points. In this case more powerful methods are needed to identify and remove the contaminating sample ([21] and [22]).

The sample could also contain several subpopulations, each following their own regression line (indeed

this is one way of viewing large scale contamination such as that in Figure 5, with points either being in the group of interest or in the contaminating subpopulation). Such a mixture of regressions greatly complicates the fitting process (see [23] for examples of such mixtures of regressions in non-astronomical examples and [22] for an astronomical application).

4 Commonly used regression techniques in astronomy

In this section we will summarise the various approaches to regression commonly used in astronomy. Generally in cases where parametric models are to be used, it is possible to label approaches as either “frequentist” or “Bayesian”. The former bases inference on the likelihood of how the data arise, while the latter works with the posterior distribution of the parameters given the data using some prior information in the model building. Consequently, the rationale behind parameter estimation differs between the two, as does the subsequent assessment of parameter uncertainty. In a frequentist setting, Maximum Likelihood Estimation (MLE) is usually preferred, that is choosing the parameter estimates which maximise the likelihood. In a Bayesian setting, parameter estimates are chosen as appropriate summaries of the posterior distribution, for example the posterior mean or the posterior mode. Other parameter estimation rationales are also in use, for example Method of Moments, Least Squares or Robust estimates; a recent overview is given by [24]. We review how some of this methodology have been used in the astronomy literature, attempting to highlight strengths and weaknesses.

4.1 Ordinary Least Squares regression

The method of fitting a regression line $y = ax + b$ by ordinary least squares regression (OLS) is extremely widespread in many disciplines ([25]). Based on the rationale of minimising the sum of squared residuals (i.e. the difference between the observed data and the values fitted to each point by the model), $S = \sum_{i=1}^N (y_i^{obs} - (b + ax_i))^2$, the parameter estimates are easily calculated as

$$\begin{aligned}\hat{a} &= \frac{\widehat{\text{Cov}}(x, y^{obs})}{\widehat{\text{Var}}(x)} \\ \hat{b} &= \bar{y}^{obs} - \hat{a}\bar{x}\end{aligned}\tag{6}$$

where we deliberately express the estimators in terms of the estimated moments of x and y^{obs} for compatibility with later estimators.

As a rationale for parameter estimation, OLS does not require any underlying distributional assumptions to be made. Finding uncertainty estimates associated with these parameter estimates does however require some such assumptions (as a minimum the mean and variance of the error structure for y^{obs}). In the case that the $\{x_i\}$ are observed without any error and y_i errors are all Gaussian, of the same size, and there is no intrinsic scatter (i.e. that the rather simplistic Equation (3) holds) then OLS is equivalent to fitting the model using Maximum Likelihood. In this case a great deal of theory exists for how the OLS estimators behave statistically. A well developed suite of diagnostic devices exists for spotting when the assumptions are violated. Diagnostic plots and diagnostic statistics followed by omission of the offending points can be used to tackle outlier problems. However as stressed by one of the anonymous referees “simple strategies like outlier detection and elimination based on diagnostic plots tend to work reliably only in simple regression with one predictor and a few outliers - but even then problems arise because little can be said about the distribution of the final parameter estimators based on such deletion procedures, so that the use of such estimators should not be encouraged.”

OLS is also not very robust to the other complications we might reasonably expect to crop up in astronomical data, Section 3. For example, when there is error on the predictor variable (i.e. x^{obs} is a noisy version of x) which is uncorrelated with the error on the response variable, then the estimate of the slope

of the regression line a is statistically biased towards zero (see, for example, [10], Chapter 4). This has an obvious negative effect when we are primarily interested in assessing scaling relations. As a result, various alternatives have been developed and we describe these in the following sections.

4.2 Weighted least squares fits

OLS minimises the sum of the squared residuals of fitting the line $ax + b$ to the data y^{obs} . If the y errors are homoscedastic (i.e. all with variance equal to σ^2), minimising the sum of the squared residuals is equivalent to minimising

$$\sum_{i=1}^N \frac{(y_i^{obs} - (b + ax_i))^2}{\sigma^2}. \quad (7)$$

When there is intrinsic scatter and the observation noise is actually heteroscedastic, the logical next step in many astronomical works is to minimise a weighted sum of residuals

$$\chi^2 = \sum_{i=1}^N \frac{(y_i^{obs} - (b + ax_i))^2}{\sigma_i^2} \quad (8)$$

where $\sigma_i^2 = \sigma_{scat}^2 + \sigma_{y,i}^2$ represents the intrinsic scatter plus the heteroscedastic measurement noise in the notation of Equation (5) and these values are assumed known. See [26] for numerical details of minimising this penalty.

Of course, we are also likely to be facing observational errors on the $\{x_i\}$, so that in fact we observe instead the $\{x_i^{obs}\}$. If the observation noise on both variables and the intrinsic scatter are statistically independent and known, one may introduce a new reweighted penalty

$$\chi^2 = \sum_{i=1}^N \frac{(y_i^{obs} - (b + ax_i^{obs}))^2}{\sigma_i^2 + a^2 \sigma_{x,i}^2}. \quad (9)$$

We stress that the standard notation χ^2 does not imply that the statistic follows the distribution of the same name. This change in weighting arises because following Equation (5),

$$\begin{aligned} y_i^{obs} &= y_i + \epsilon_{y_i} \text{ where } \epsilon_{y_i} \sim N(0, \sigma_{y,i}^2) \\ &= (ax_i + b + \epsilon_{scat}) + \epsilon_{y_i} \text{ where } \epsilon_{scat} \sim N(0, \sigma_{scat}^2) \\ &= a(x_i^{obs} - \epsilon_{x_i}) + b + \epsilon_{scat} + \epsilon_{y_i} \text{ where } \epsilon_{x_i} \sim N(0, \sigma_{x,i}^2) \\ \text{so } Var(y_i^{obs}) &= a^2 \sigma_{x,i}^2 + \sigma_i^2 \text{ where as before } \sigma_i^2 = \sigma_{scat}^2 + \sigma_{y,i}^2. \end{aligned} \quad (10)$$

The optimisation is complicated by the a^2 term on the denominator which makes the problem nonlinear, [26] provides a suitable numerical optimisation algorithm known as FitEXY. Minimisation of this reweighted penalty requires that the $\{\sigma_i^2\}$ and $\{\sigma_{x,i}^2\}$ are known. Weighted least squares fits cannot address an unknown intrinsic scatter by including the parameter when minimising over all the unknown parameters (if σ_{scat}^2 is unknown, then doing this, the minimal χ^2 obviously occurs for $\sigma_{scat}^2 \rightarrow \infty$). [27] points out that finding associated statistical properties of this estimator can be achieved via bootstrapping.

4.3 Maximum Likelihood Estimation

Putting a greater emphasis on parametric modelling than does OLS, Maximum Likelihood Estimates (MLEs) are those parameter estimates which maximise the likelihood of the observed data. They are much favoured by statisticians not least because of the wealth of associated theory which yields (asymptotic) sampling distributions in many cases and thus interval estimates and hypothesis tests.

In several of the scenarios considered in the previous two sections, MLE and OLS or weighted least squares estimates of the regression parameters a and b would coincide. For example, reconsidering the case where the $\{\sigma_i^2\}$ are known, there is no observation noise on the $\{x_i\}$, and the Normality assumptions of Equation (5) hold, then the likelihood for for a and b is

$$L(a, b) = \prod_{i=1}^N \frac{1}{\sqrt{2\pi\sigma_i^2}} \exp\left(-\frac{(y_i^{obs} - ax_i - b)^2}{2\sigma_i^2}\right). \quad (11)$$

It is clear that the maximisers of Equation (11) are also the minimisers of χ^2 defined in Equation (8) ([28]).

The situation is more complicated if the intrinsic scatter, σ_{scat}^2 , has to be determined from the data or if there is observation noise on the $\{x_i\}$; this latter errors-in-variables regression has been considered in the statistics literature; for example, [29], Chapter 3, and [30], Chapter 12, have nice discussions of different approaches to the problem. In the case where the errors for both x and y are normal and homoscedastic, the complete likelihood can be written

$$L(a, b, \{x_i\}, \sigma_x^2, \sigma_y^2) = (2\pi\sqrt{\sigma_x^2\sigma_y^2})^{-N} \exp\left(-\frac{\sum_{i=1}^N (x_i^{obs} - x_i)^2}{2\sigma_x^2}\right) \exp\left(-\frac{\sum_{i=1}^N (y_i^{obs} - ax_i - b)^2}{2\sigma_y^2}\right) \quad (12)$$

where σ_x^2 represents the variance of the x error and σ_y^2 represents the sum of σ_{scat}^2 and the common variance for the y observations. They point out that by taking each $x_i = x_i^{obs}$ and letting $\sigma_x^2 \rightarrow 0$, the likelihood can be made arbitrarily large. As a result, maximum likelihood tends only to be performed after making additional assumptions about the variances, most commonly that $\sigma_x^2 = \lambda\sigma_y^2$ where λ is a known positive constant (although this assumption is not without its problems, [31]). Alternatively, if we were to assume known heteroscedastic variances $\sigma_{x,i}^2$ and $\sigma_{y,i}^2$, the corresponding likelihood would be

$$L(a, b, \{x_i\}, \sigma_{scat}^2) = \frac{(2\pi)^{-N}}{\prod_{i=1}^N \sqrt{\sigma_{x,i}^2(\sigma_{y,i}^2 + \sigma_{scat}^2)}} \exp\left(-\frac{\sum_{i=1}^N (x_i^{obs} - x_i)^2}{2\sigma_{x,i}^2}\right) \exp\left(-\frac{\sum_{i=1}^N (y_i^{obs} - ax_i - b)^2}{2(\sigma_{y,i}^2 + \sigma_{scat}^2)}\right) \quad (13)$$

which could be maximised numerically over the $N + 3$ unknown parameters, although again it is not clear whether the known variances assumption is justifiable. Equation (13) has the unappealing property that the number of unknowns, $N + 3$, increases as the number of data points, $\{x_i^{obs}, y_i^{obs}\}_{i=1}^N$, increases. In particular, this means that the usual asymptotic distributional results for MLEs do not hold.

4.4 Robust estimation

Parameter estimation can be affected by outliers and other violations of parametric assumptions. Robustness to outliers and to some aspects of the Normality assumptions can be introduced by a switch from *least squares* to *least absolute deviations*, replacing the standard sum of squares by (in its simplest case)

$$S = \sum_{i=1}^N |y_i^{obs} - (b + ax_i)|. \quad (14)$$

This form is quite commonly used in astronomy, being offered in [26]; see also [32] for a witty introduction.

The fitted value \hat{b} is here the median of the $y_i^{obs} - (b + ax_i)$ and the estimate of the slope can be found numerically as the solution of the equation

$$0 = \sum_{i=1}^N x_i \text{sign}(y_i^{obs} - (\hat{b} + ax_i)). \quad (15)$$

(There may not be a unique solution to this problem.) Least absolute deviations regression is quite robust against unusual y_i^{obs} but it does not cope so well with unusual x_i values (high leverage points) and can be quite unstable with regard to small changes in the $\{x_i\}$. However it is just one possible robust approach and this is an active field of research, see for example [33], Chapter 7.

4.5 Bivariate Correlated Errors and Intrinsic Scatter (BCES)

In 1996 [9] proposed a widely applicable extension of OLS, known as BCES. It considers regressions with heteroscedastic and even correlated errors on both axis as well as an intrinsic scatter. Again the assumption is made that the measurement error variances and covariances are known, although they may vary from point to point, and importantly they may be a function of the response and predictor variables. The BCES estimator extends OLS by considering the usual estimates in terms of the moments of the bivariate distribution of x and y , Equation (6), and then expressing these moments in terms of the moments of the observed x^{obs} and y^{obs} and the known measurement variances. In analogy with Equation (6), the BCES estimates of slope and intercept when regressing y on x are

$$\begin{aligned}\hat{a} &= \frac{\widehat{\text{Cov}}(x^{obs}, y^{obs}) - \frac{1}{N} \sum_{i=1}^N \sigma_{xy,i}^2}{\widehat{\text{Var}}(x^{obs}) - \frac{1}{N} \sum_{i=1}^N \sigma_{x,i}^2} \\ \hat{b} &= \bar{y}^{obs} - \hat{a} \bar{x}^{obs}\end{aligned}\tag{16}$$

where $\sigma_{xy,i}^2$ is the known covariance between $\epsilon_{x,i}$ and $\epsilon_{y,i}$ and $\sigma_{x,i}^2$ is the known variance of $\epsilon_{x,i}$ (as defined by Equation (5)). These estimates are referred to as the ‘‘Moment-based corrected estimators’’ in [10], Chapter 4, where fuller discussion is given regarding their properties. Asymptotically, the slope and intercept estimators are shown by [9] to have Gaussian sampling distributions and so confidence intervals can be estimated. As an alternative, BCES also assesses the fitting errors using bootstrap ideas (repeatedly resampling from the observed data to form an empirical sampling distribution of the estimators). See the original paper for more complete details.

Equation (16) provides point estimates for the regression of y on x . [9] also derive estimates for when the regression of x on y is preferred. As the two resulting lines will not be equal, the BCES bisector is also defined as the bisector of the two.

BCES addresses some of the difficulties arising in scaling relations in astrophysics, namely errors on measurements which are potentially correlated as well as being functions of the true x and y . However, problems related to outliers, data structure, upper-limits and selection effects are not addressed by this methodology, and in small data sets non-Normality of the data may be an issue for exact confidence intervals. Code to implement these estimators is available via

<http://www.astro.wisc.edu/~mab/archive/stats/stats.html>.

4.6 Astronomy Survival Analysis (ASURV)

In the wider world of statistics, there are many application areas in which data are censored and the field of survival analysis has developed to deal with such data (see [34] for example). As the name perhaps suggests, survival analysis tends to deal with cases where observations can only be made when the subject survives more or less time than a certain observation date. As such, the analogy with flux or other attribute limited selection is quite clear. The analogy is not perfect however when we are thinking about upper/lower limits or selection function, because these are stochastic (the inclusion/exclusion occurs with some probability), while censoring is deterministic.

[35] and [36] introduced the astronomical community to these ideas thereby allowing astronomers to perform regression in the presence of upper/lower limits (following the paper [37] on a similar theme for univariate problems). [35] leads the reader through a series of statistical procedures in the presence of censoring, of which we will concentrate here on regression with the assumption of upper-tail censoring on both variables and a known number of potential observations. The suggested procedure begins by finding a nonparametric estimate of the joint distribution of the two variables. To do this, the data are first binned on each variable separately, including a bin for the censored values. Then considering the intersection of the two sets of bins, four distinct classes emerge: points for which both measurements are available, points for which only one variable is available with the other censored (the two cases), and points for which

both values are censored. Based on counts of the numbers of points in each class, [35] derives Maximum Likelihood estimates of the probability of each bin combination. This stage does not make any parametric assumptions about how the data are distributed. Finally, given the estimated joint distribution, the moments of the distribution can be found and used in the usual OLS formulations, Equation (6). See the original paper for more complete details.

[36] reviews the methodology of [35], adding two further approaches. In the first, data are assumed only to be censored on the response variable, and a distributional assumption of Normality is made for the response variable then using the EM algorithm [38] to impute the censored values for use in a Maximum Likelihood approach. In the second, a nonparametric approach is taken, relaxing the Normality assumption but again only assuming censoring on one variable, making it perhaps less widely applicable than the approach of [35]. The paper compares the various approaches via simulation studies and on several astronomical applications. A useful resource written by some of the authors of this paper, amongst others, is code to implement these estimators, available at <http://astrostatistics.psu.edu/statcodes/asurv> and described in [39].

The explicit handling of censoring greatly extends the range of regression problems which can be tackled appropriately, as does the nonparametric approach of some of the methods. However some limitations remain; there is not currently provision for incorporating intrinsic scatter nor heteroscedastic error structure, nor the other common features of astronomical data in Section 3. In particular, ASURV only considers a specific type of upper limit censoring, which is a sharp upper limit. As already mentioned, the most usual case in astronomy is a soft, probabilistic, threshold, one in which also some objects below the threshold may be observed while some objects above the threshold will be missed.

4.7 Errors-in-variable Bayesian regression

Bayesian regression started to receive significant attention in the astronomical community after the publication of [40], which is a brief summary of the relevant content in [41], and the errors-in-variable model of [42]. The important differences for the practitioner between Bayesian and non-Bayesian approaches lie in the model specification and interpretation of results. In terms of the former, a Bayesian approach takes the usual question “How did the data I observed arise?” and adds the new question “What do I know about the parameters even before I collect any data?”. Effectively it asks the practitioner to quantify their uncertainty about the parameters in the form of a prior distribution (which may be either very precise or, more commonly, very vague). This is combined with the usual likelihood for how the data arise via Bayes’ theorem to form a posterior distribution which now quantifies our uncertainty about the parameter having observed data. In a mathematical sense, the posterior distribution is simply proportional to the product of the likelihood function and the prior distribution. Summarising the posterior by its location (mean, median, mode, etc) quantifies the parameter value; its spread, e.g. the interval that includes 68% of it, quantifies the parameter uncertainty. On the practical side, there are now a number of Bayesian packages which allow the user to specify relatively general models without needing to compute the posterior in closed form (i.e. as a single mathematical expression whose derivation is often difficult). Amongst them, perhaps the most notably are BUGS [43] and JAGS [44].

Despite the philosophical differences, since a Bayesian approach and fitting by Maximum Likelihood share a common model for how the data arise, it is often the case that, numerically, the two sets of resulting point estimates can be quite close, especially if there is a lot of informative data or if the prior information is weak. This is entirely positive. Where a Bayesian analysis may really help is when perhaps we have strong prior information or wish to explore the uncertainty associated with relaxing some condition required for Maximum Likelihood estimation (for example, the constant ratio of variances assumption). It may also permit some dimension reduction if the latent variables $\{x_i\}$ are not of interest by integrating them out of the posterior distribution analytically, as is done by [40]. For example, considering Equation (13), the posterior

for just a, b, σ_{scat}^2 can be expressed

$$\begin{aligned} p(a, b, \sigma_{scat}^2 | \{x_i^{obs}, y_i^{obs}\}) &= \int_{\{x_i\}} p(a, b, \{x_i\}, \sigma_{scat}^2 | \{x_i^{obs}, y_i^{obs}\}) d\{x_i\} \\ &\propto \int_{\{x_i\}} L(a, b, \{x_i\}, \sigma_{scat}^2) p(\{x_i\}, a, b) d\{x_i\} \end{aligned} \quad (17)$$

where $p(\{x_i\}, a, b)$ is the joint prior and the integration is over the N dimensional latent variables. Obviously this dimension reduction approach will only be feasible in certain analytically tractable cases. When analytic dimension reduction is not an option, numerical marginalisation is required, either directly by numerical integration or indirectly by Monte Carlo methods.

To illustrate the Bayesian approach, a version of the errors-in-variable regression model assuming known $\{\sigma_{x,i}^2\}$ and $\{\sigma_{y,i}^2\}$ takes the usual likelihood equations

$$\begin{aligned} x_i^{obs} &\sim N(x_i, \sigma_{x,i}^2) && \text{Gaussian errors on } x^{obs} \\ y_i^{obs} &\sim N(y_i, \sigma_{y,i}^2) && \text{Gaussian errors on } y^{obs} \\ \text{where } y_i &\sim N(ax_i + b, \sigma_{scat}^2) && \text{Gaussian intrinsic scatter around a straight line for } y \end{aligned} \quad (18)$$

and adds the equations specifying the additional question ‘‘What do I know about the parameters even before I collect any data?’’, for example, we could specify that independently

$$\begin{aligned} x_i &\sim U(-10^4, 10^4) && \text{Uniform population structure for } x_i, i = 1, \dots, N \\ \sigma_{scat}^2 &\sim InvGam(0.01, 0.01) && \text{Inverse Gamma prior on scatter} \\ a &\sim t_1 && \text{Student's t on slope, equivalent to a uniform on angle} \\ b &\sim N(0, 10^4) && \text{Gaussian prior on intercept.} \end{aligned} \quad (19)$$

(The choice of an Inverse Gamma prior for the variance term is quite common but is not without criticism, [45]. The numerical values in the uniform prior are meant to indicate realistic limits for a particular application rather than being general purpose.) Precise information could be introduced for particular applications. For example we may know from previous analyses that the slope is $\pi \pm 0.1$, and in such a case we could use $a \sim N(\pi, 0.1^2)$; the prior is one way to take advantage of the work of previous generations of researchers. Code to implement the error-in-variable Bayesian regression is given in the Appendix. Other common features of astronomical data can be addressed, as we detail in Section 6.

Turning to one of the other uses of regression mentioned in Section 2, prediction, before data z are collected (or even considered), the distribution of predicted values \tilde{z} can be expressed as

$$p(\tilde{z}) = \int p(\tilde{z}, \theta) d\theta = \int p(\tilde{z}|\theta) p(\theta) d\theta. \quad (20)$$

These two equalities result from the application of probability definitions, the first is simply that a marginal distribution results from integrating over a joint distribution, the second is Bayes’ rule. If some data z have been already collected for similar objects, we can use these data to improve our prediction for \tilde{z} . For example, if mass and richness in clusters are highly correlated, one may better predict the cluster mass knowing its richness than without such information simply because mass shows a lower scatter at a given richness than when clusters of all richnesses are considered (except if the relationship has slope exactly equal to $\tan k\pi/2$, with $k = 0, 1, 2, 3$). In making explicit the presence of such data, z , we rewrite Equation (20) conditioning on z

$$p(\tilde{z}|z) = \int p(\tilde{z}|z, \theta) p(\theta|z) d\theta. \quad (21)$$

The conditioning on z in the first term in the integral simplifies because z and \tilde{z} are considered conditionally independent given θ , so that this term becomes $p(\tilde{z}|\theta)$. The left hand side of the equation is called the

posterior predictive distribution for a new unobserved \tilde{z} given observed data z and model parameters θ . Its width is a measure of the uncertainty of the predicted value \tilde{z} , a narrower distribution indicating a more precise prediction. Examples are given in Section 5.

5 Performance comparisons

In this section we consider existing and new comparisons of some of the different regression techniques. Most comparisons tend to use relatively simple simulated data sets because many of the regression techniques do not address more than a few of the features of astronomical data listed in Section 3. We split our review into performance in estimating the regression and performance in prediction. We have not included ASURV in the comparisons because it addresses only censoring of all the possible data complications and this is relatively uncommon in astronomy, which deal instead mostly with a soft, probabilistic, threshold.

5.1 Estimating the regression parameters

[27] compares performance in recovering the regression parameters for OLS, BCES and FitEXY and a likelihood model he calls the Gaussian structural model proposed in that paper. For OLS and FitEXY poor performances might be anticipated because they are applied outside their range of validity since the simulated data has heterogeneous errors on both x and y (not addressed by OLS) and a unknown intrinsic scatter (not addressed by FitEXY). In finding the Maximum Likelihood Estimates based on the Gaussian structural model he compares asymptotic theory to derive uncertainty estimates with a semi-Bayesian approach drawing samples from the associated posterior when using very weak priors. [27] found that OLS returns slopes which are statistically biased towards zero, in agreement with [9], while BCES and FitEXY return intrinsic dispersions which are systematically wrong. This is unsurprising for FitEXY and OLS since they do not address the simulated case (we emphasise that FitEXY allows an intrinsic scatter only if known). The Gaussian structural model in its semi-Bayesian approach (ignoring the prior when computing the point estimate of the parameters, but using it to compute their uncertainties) outperforms the other methods, including BCES.

[18] compares two methods only, BCES and the errors-in-variable Bayesian model [42] of Section 4.7. In this case, the comparison uses models within the range of validity, generating 1000 samples of 25 data points drawn from a linear regression with slope $a = 5$, an intrinsic scatter $\sigma_{scat}^2 = 1$, and homogeneous Gaussian errors with $\sigma_x^2 = 1$ and $\sigma_y^2 = 0.4^2$. These parameters are chosen to approximate X-ray luminosity vs velocity dispersion of clusters of galaxies e.g. [46]. Three examples are shown in Figure 6. [18] finds that BCES sometimes estimates the slope parameter very poorly (see the right hand panel in Figure 6 for an example and the left hand panel in Figure 7 for an ensemble view). When BCES does estimate the slope poorly, it does also return a much larger estimated measure of error, right hand panel in Figure 7. On average over the 1000 simulations, the Bayesian approach has a smaller measure of error than BCES.

Computationally, the costs of the different techniques vary considerably, OLS being the cheapest and the Bayesian errors-in-variables the most expensive as it requires Markov chain Monte Carlo methods (MCMC). In this later case, depending on the size of the data set, the cost may be up to a few minutes or hours depending on the complexity of the model rather than a few seconds.

5.2 Prediction

Turning to a comparison of prediction accuracy, we consider a simulation study involving a simpler scenario than that in the previous section. We generate 100 values of x_i from a non-central scaled Student-t distribution with 10 degrees of freedom, location 0.1, and scale 1.1. These x_i are perturbed by homoscedastic Gaussian noise with $\sigma_x^2 = 1$ to give 100 x_i^{obs} . The regression line takes the form $y = x$ with no intrinsic scatter, and these y_i are also perturbed by homoscedastic Gaussian noise with $\sigma_y^2 = 1$ giving 100 y_i^{obs} . The resulting $\{x_i^{obs}, y_i^{obs}\}$ pairs are used as the data for the errors-in-variable Bayesian model, OLS, weighted

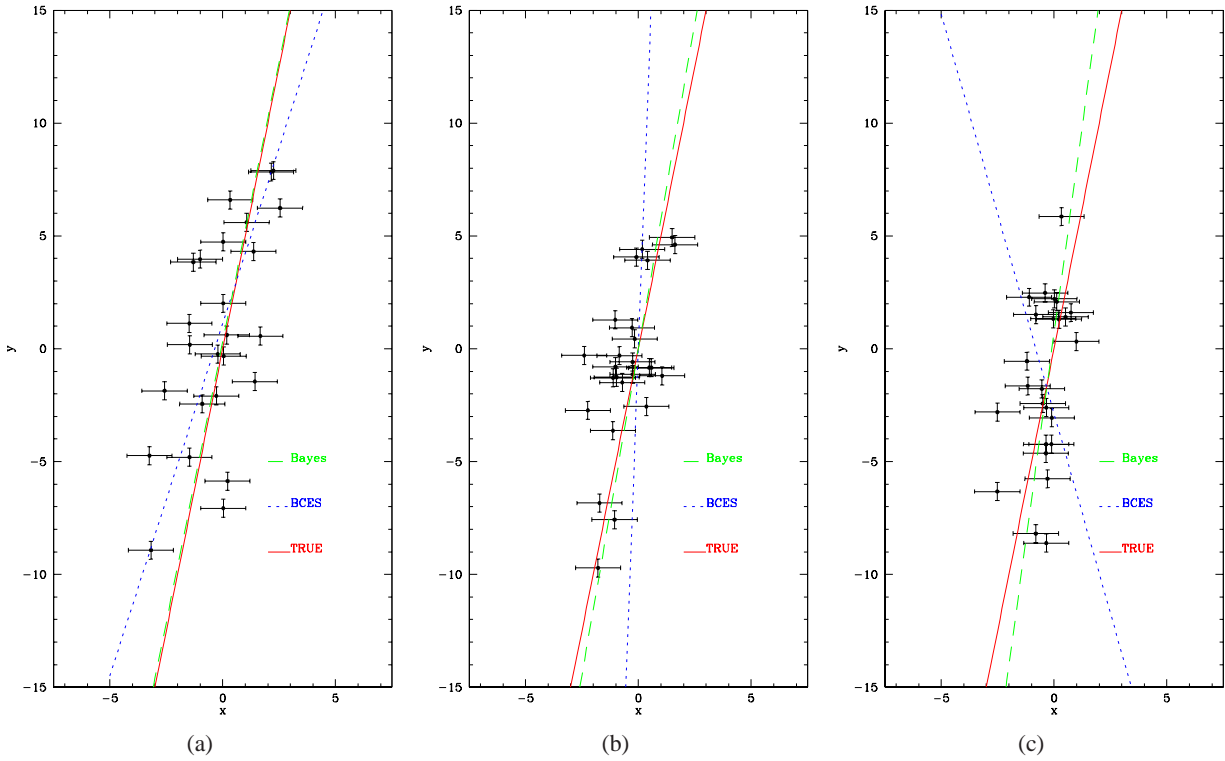


Figure 6: Three simulated data sets each of 25 points, showing true trends from which the data are generated in red, the trend recovered by BCES in blue, and the mean Bayesian estimate in green. In 1000 simulations, BCES results performed worse than those shown in the central and right panels about 10% of the times. The simulations are meant to mimic the $L_X - \sigma$ scaling of galaxy clusters (from [18]).

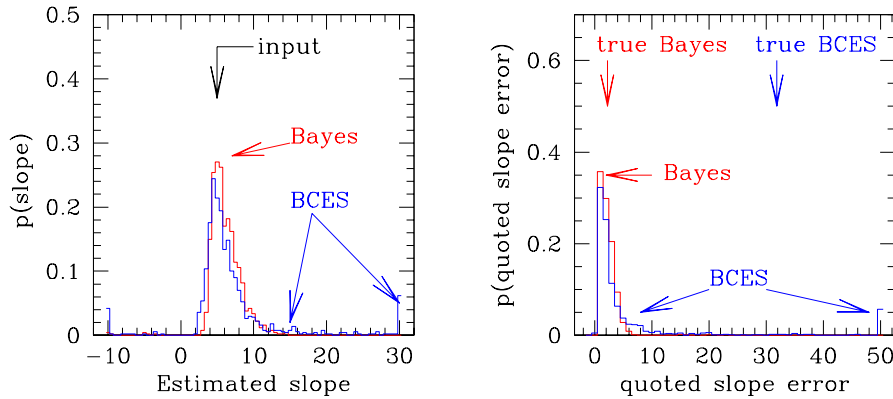


Figure 7: Comparison between BCES (blue) and the Bayesian approach (red) for a linear regression problem (from [18]) using 1000 simulations of a sample of 25 objects. *Left panel:* Histogram of point estimates of the slope parameter, note that the extreme bins represent ≤ -10 and ≥ 30 . In approximately 12% of the simulations, BCES returns significantly wrong estimates, the fit associated with one of these is plotted in the right hand panel of Figure 6. *Right panel:* Histogram of estimated variability of slope estimates; for BCES this is the returned standard error, for the Bayesian approach it is the returned standard deviation of the posterior mean for the slope. Note that estimates larger than 50 are binned for display purposes at 50. The two arrows denote the standard deviations calculated from the 1000 simulations of the observed differences between the true and the estimated slopes.

least squares, BCES and MLE (in all cases the variances of the noise are assumed known). The likelihood for the unknowns $a, b, \{x_i\}$ based on the observations $\{x_i^{obs}, y_i^{obs}\}$ can be written

$$L(a, b, \{x_i\}) = \frac{(2\pi)^{-N}}{\prod_{i=1}^N \sqrt{\sigma_x^2 \sigma_y^2}} \exp\left(-\frac{\sum_{i=1}^N (x_i^{obs} - x_i)^2}{2\sigma_x^2}\right) \exp\left(-\frac{\sum_{i=1}^N (y_i^{obs} - ax_i - b)^2}{2\sigma_y^2}\right) \quad (22)$$

Noting that for MLE for this experiment the likelihood has 102 unknown parameters. We follow [40] in using the likelihood

$$L(a, b) = \frac{\sqrt{2\pi}^{-N}}{\prod_{i=1}^N \sqrt{\sigma_y^2 + a^2\sigma_x^2}} \exp\left(-\frac{\sum_{i=1}^N (y_i^{obs} - ax_i^{obs} - b)^2}{2(\sigma_y^2 + a^2\sigma_x^2)}\right) \quad (23)$$

which corresponds to integrating out the $\{x_i\}$. Notice the correspondence between the exponential term in this equation and Equation (9), although they differ in that Equation (23) also has an a dependence in the leading non-exponential term. Therefore, when there are errors on the predictor quantity, weighted least squares is not the MLE estimate.

For the Bayesian errors-in-variable model we retain the $\{x_i\}$ in the model and so will need to assume a prior population model for them. Retaining the $\{x_i\}$ in the model does increase the computational cost although as a byproduct it does also generate estimates of the $\{x_i\}$ which might be useful in some applications. In some astronomical problems, the x data structure is fairly well known (e.g. from previous experiments or from theory). If this were the case here, the prior would be

$$x_i \sim t_{10}(0.1, 1.1^2), \quad i = 1, \dots, 100 \quad (24)$$

since this is actually the true population model. Of course it may well be the case that we do not have such a high level of prior knowledge and so we also consider an alternative prior

$$x_i \sim N(0, 1^2), \quad i = 1, \dots, 100 \quad (25)$$

which has a difference in location and scale as well as a lighter tail behaviour as an example of possible mismatch between the true data structure and what we know about it. This prior is still relatively informative; it might perhaps be arrived at in a not strictly Bayesian sense by looking at a histogram of the 100 x_i^{obs} values. Finally, we also consider a less informative prior, with parameters to be determined at the same time as the other regression parameters; we have adopted a Normal prior with parameters treated as additional unknowns

$$x_i \sim N(\mu_{prior}, \sigma_{prior}^2), \quad i = 1, \dots, 100 \quad (26)$$

with weak hyperpriors on the parameters

$$\mu_{prior} \sim N(0, 10^4) \quad (27)$$

$$1/\sigma_{prior}^2 \sim U(0, 10). \quad (28)$$

Using the observed data, the Bayesian model makes predictions of y, \tilde{y} , for new x^{obs} using Equation (21). The non-Bayesian techniques have point estimates of the slope \hat{a} and intercept \hat{b} using the original 100 points, and these are used to give predictions $\tilde{y} = \hat{a}x^{obs} + \hat{b}$ for new x^{obs} . To assess performance, 10000 new x_i^{obs} values are simulated from the model and for each we calculate the residual between the predicted \tilde{y}_i and the actual y_i . Figure 8 plots these residuals against the value of x^{obs} for the various different fitting algorithms (binning the results in small x^{obs} intervals to aid visualisation). Notice that we plot the residuals against x^{obs} rather than against x ; although this induces a correlation with the residuals for some methods, it is actually the performance for an observed x^{obs} rather than an unobserved x which may be of interest to practitioners. This also emphasises the point made by [29], Chapter 2, that homoscedastic measurement

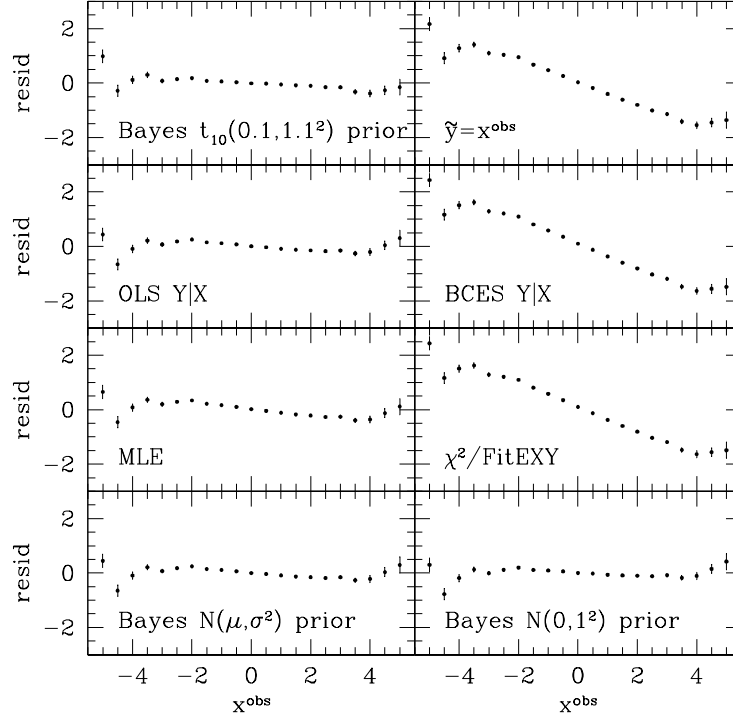


Figure 8: Performance of the various approaches in predicting the true value y given x^{obs} . Each point show the average residual per small bin of x^{obs} . The error bars indicate the standard error of the mean residuals.

error is less of a problem for prediction than it is for parameter estimation because one is predicting on the basis of x^{obs} and not x and thus methods which ignore the distinction are not penalised to the same extent. In this simulation, that makes OLS a competitive standard.

Running through the results as laid out in Figure 8:

Top row, left Bayes regression with a $t_{10}(0.1, 1.1^2)$ prior performs very well with small residuals across the entire range of x^{obs} as is to be expected given that the correct model is being fitted. The point estimates of the parameters themselves are 1.09 and 0.00 for the slope and intercept respectively.

Top row, right Suppose that one naively attempts to predict \tilde{y} by $\tilde{y} = x^{obs}$, in effect making use of the knowledge that $y = x$ but ignoring the noise structure. The residual in this case is the perturbation $x - x^{obs}$, i.e. a $N(0, 1)$ value in this example, however it is as a result negatively correlated with x^{obs} so that the largest residuals occur at the extremes of x^{obs}

Second row, left OLS generates better predictions than the naive estimate. It achieves this better performance by underestimating the true slope, returning an estimated slope of 0.65 in place of the input 1 and an intercept of 0.02 in place of 0, in agreement with [9] and Section 2. Feeling that this fitted line is not steep enough to capture the data trend (see discussion on Figure 1 for a related case), some astronomical papers average this slope with the one derived by swapping x^{obs} with y^{obs} . However while this may be more appropriate for parameter estimation, it is suboptimal for prediction. In this case this gives a new fitted line with a slope near to one, as in our $\tilde{y} = x^{obs}$ case, and consequently the performance of this averaged OLS method is close to the naive estimator case.

Second row, right Predicted \tilde{y} values computed using the BCES method are similar to those using the naive $\tilde{y} = x^{obs}$ method. Comparing Equation (16) when $\sigma_{xy,i}^2 = 0$ with Equation (6) it is apparent that in improving the estimates of the slope and intercept, the prediction performance is degraded.

Table 1: Mean residuals at various values of x^{obs}

	$x^{obs} = -5$	$x^{obs} = -3$	$x^{obs} = -1$	$x^{obs} = 1$	$x^{obs} = 3$	$x^{obs} = 5$
Bayes $t_{10}(0.1, 1.1^2)$ prior	0.98	0.06	0.04	-0.07	-0.17	-0.15
x^{obs}	2.16	1.10	0.47	-0.40	-1.14	-1.36
OLS	0.44	0.07	0.11	-0.09	-0.15	0.30
BCES	2.43	1.29	0.58	-0.37	-1.19	-1.49
MLE	0.65	0.20	0.17	-0.12	-0.26	0.11
χ^2/FitEXY	2.43	1.29	0.58	-0.37	-1.19	-1.49
Bayes $N(\mu, \sigma^2)$ prior	0.45	0.07	0.11	-0.09	-0.16	0.29
Bayes $N(0, 1^2)$ prior	0.30	-0.01	0.09	-0.06	-0.08	0.42

Any uncertainty associated with the predictions for a fixed value of x^{obs} is associated purely with the uncertainty of x corresponding to this x (and thus the corresponding y). This is not an issue for between-method comparison and so is omitted.

Third row, left MLE using Equation (23) returns reasonable predictions.

Third row, right χ^2/FitEXY , Equation (9) performs less well than MLE because Equation (23) has a leading term missing in Equation (9).

Bottom row, left and right Bayesian errors-in-variables regression with either a $N(\mu, \sigma)$ prior for the $\{x_i\}$ or a $N(0, 1)$ prior performs almost as well as the Bayesian model using the true distribution as a prior, showing that an accurate knowledge of the prior is not necessary to achieve good performance in this example.

In addition to Figure 8, Table 1 lists residuals at a few points ($|x^{obs}| = 1, 3, 5$) for all our comparison performances. To summarise for this example the methods based on sound statistical models applied appropriately (MLE, Bayesian regression) outperform BCES and weighted least squares. OLS also does well here paradoxically because of its sheer simplicity. Of these methods, the Bayesian regression also generates estimates for the $\{x_i\}$, if these are required, as well as reliable estimates of the regression parameters (unlike OLS). If we were talking about predicting observationally expensive masses (\tilde{y}) from observationally parsimonious mass proxies (x^{obs}), such as richness or X-ray luminosity, non-Bayesian fitting models are either inaccurate in predicting the trend between mass and proxy (i.e. return an incorrect slope of the y vs x relation) or perform very badly in predicting masses from observed values of mass proxies. The Bayesian fit estimates the slope accurately and provides well predicted masses, and so may achieve better results for the same costly telescope time, albeit at greater computational cost.

6 Including more features of astronomical data in Bayesian regression

Section 3 listed many common features of astronomical data. In this section we consider how we might expand the Bayesian errors-in-variable model to include some of these features and others. In some cases, it is a question of changing the likelihood of how the data arise. In others, it is the prior which must change. Notice that in the former case, a non-Bayesian approach might also work with this same modified likelihood, usually at the cost of a more complex fitting by Maximum Likelihood.

- Heteroscedastic errors on both x and y are already accounted for in the errors-in-variable model. However so far they have been assumed known. Very often, uncertainties are not perfectly known because of the complexity of determining them (based on properties of the mechanism by which the data are obtained, rather than by a statistical repeat sampling approach). [3] extends the simple example model to allow for this uncertainty. Denoting the value for the variance suggested by the physics by $s_{y,i}^2$, a prior is constructed which reflects both the positivity of $\sigma_{y,i}^2$ and the accuracy of

$s_{y,i}^2$:

$$\sigma_{y,i}^2 \sim \frac{s_{y,i}^2}{\nu} \chi_{\nu}^2. \quad (29)$$

The degrees of freedom of the distribution, ν , control the spread of the distribution, with large ν meaning that quoted variances will be close to the true variances. [3] uses $\nu = 6$ to quantify with 95% confidence that quoted standard deviations are correct up to a factor of 2 (i.e. $\frac{1}{2} < \frac{\sigma_{y,i}}{s_{y,i}} < 2$). Notice that it is not possible to put a flat prior on these terms since there is a lack of identifiability associated with partitioning the variability of the y_i^{obs} between $\sigma_{y,i}^2$ and σ_{scat}^2 .

- **Intrinsic scatter.** This is taken to be Normal in the standard errors-in-variable model, but it could readily be replaced with something more suitable for the particular application, for example with a Cauchy distribution, $y_i \sim Cauchy(ax_i + b, \sigma_{scat}^2)$ if the scatter between x and y is thought to be exceptionally heavy tailed (the Cauchy distribution is equivalent to the t on 1 degree of freedom). An application is provided by the computation of the color offset of stellar locii ([47]): allowing heavier-than-Gaussian tails one may account for contamination by QSO and objects with corrupted photometry.
- **Non-ignorable data collection and selection effects.** In this case, the problem is the same for Bayesian and non-Bayesian methods since it is the likelihood of the observed data which is affected. [48] nicely describes a modified likelihood taking into account selection effects. Suppose we introduce a new binary variable D_i for observation i where $D_i = 1$ if i is observed and zero otherwise and D_i depends only on the value of the underlying y_i . The likelihood of observing a value y_i^{obs} , denoting other parameters of the model collectively by θ , can then be expressed

$$f(y_i^{obs} | D_i = 1, y_i, \theta) = \frac{f(D_i = 1 | y_i) f(y_i^{obs} | y_i, \theta)}{\int_{-\infty}^{\infty} f(D_i = 1 | z) f(z | y_i, \theta) dz} \quad (30)$$

where $f(y_i^{obs} | y_i, \theta)$ is the usual likelihood when there are no selection effects (for example, $N(y_i, \sigma_{y,i}^2)$ in the usual errors-in-variable model) and $f(D_i = 1 | y_i)$ is the sample selection function (strictly related to the sky coverage). The integral in the denominator of Equation (30) gives the probability of detection given the values y_i and θ . Working with this likelihood complicates both Bayesian and non-Bayesian methods.

An application is provided by the $L_X - T$ relation of Figure 3, where the simulated data are generated from the blue line, then selected according to the XMM-LSS selection function [12]. In this example, the probability that an object enters the sample, $f(D_i = 1 | y_i)$, changes smoothly from zero to one depending on luminosity and temperature as it does with real data; it does not go abruptly from zero to one at a given threshold as assumed in survival analysis. Using the modified likelihood, the input regression can be estimated (see [11] for details).

- **Data structure and non-uniform population.** This problem is readily addressed in the Bayesian setting by choosing the most appropriate prior for the population. For example when dealing with the source of the Malmquist bias in faint object measurements, it might be appropriate to use a common power law, as done in the case illustrated in Fig. 4 ([18], see also [49]).
- **Non-Gaussian data and upper limits.** Non-Gaussian data requires a change of likelihood model for x^{obs} , y^{obs} , or perhaps both. As an example, consider the application presented in [3], illustrated in Figure 2(a). Here the observations on the x axis are the logs of count data where it might be expected that count data are Poisson distributed: If we denote the counts by $\{n_i^{obs}\}$, then a slight simplification of the model used in [3], would be

$$n_i^{obs} \sim \mathcal{P}(x_i) \quad \text{Poisson error on observation with rate } x_i$$

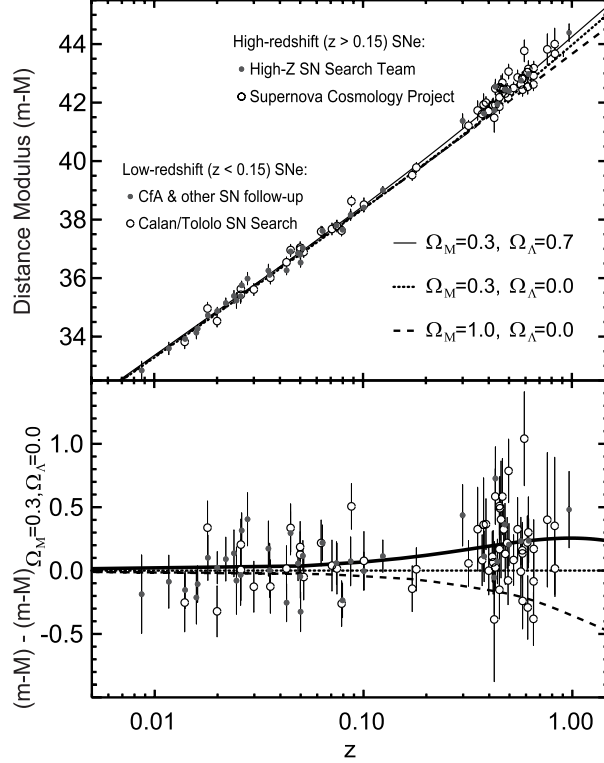


Figure 9: Hubble diagram for supernovae. The object flux weakens (the distance modulus, $m - M$, becomes greater) in a way that depends on the geometry of the Universe (from [54]) and leads to the recent Nobel prize winning discovery of the Dark Energy. With kind permission from Springer.

$$\begin{aligned}
 x_i &\sim U(0, 10^4) && \text{A weak prior on the underlying positive rate} \\
 y_i &\sim N(a \log(x_i) + b, \sigma_{scat}^2) && \text{Gaussian regression prior on the response } y_i.
 \end{aligned} \tag{31}$$

We emphasize that n_i^{obs} is a discrete count while x_i is the underlying continuous rate.

Upper limits are automatically accounted for by the above change. Suppose, for example, we are dealing with photons and we detected zero photons, $n_i^{obs} = 0$, from a source i of intensity x_i . This value gives an upper limit to the source intensity (2.3 at 90% confidence).

- **Circularity arguments.** Very often in order to take a measurement aimed at constraining a parameter, we need to know the parameter before performing the measurement, leading to a circular reasoning. For example, if one wants to infer cosmological parameters from clusters of galaxies, we need scaling relations (to relate the observable quantities to mass) and measurements performed in standard apertures (say r_{500}). However, the angular size of the latter depends on the cosmological parameters one is aiming to determine. If instead supernovae are used for the same goal (and cosmological constraints come from the scaling between their distance modulus and redshift, see Figure 9), then one needs to know how their absolute luminosity should be corrected (peak luminosity is brighter for slow fading supernovae, [50]), a correction which in turn requires knowledge of cosmological parameters, which is exactly what one wishes to infer. The Bayesian solution is to model the dependence of the measurements on the cosmological parameters and fit them all at once, see [51], [52] and [53].

Other complexities, such as non-linear regressions, extra-Poisson fluctuations and contamination have been already successfully dealt with in astronomical works using Bayesian methods ([3], [13], [22], [21])

We note that on the computational side, accounting for these and other complications is relatively pain free in terms of statistical effort (if not in terms of computing time) since converting the written symbolic

equations into code and then implementing it is undertaken by Bayesian tools such as JAGS. Readers may refer to the Appendix and [3], [11], [13], [49], [53], and [55] for examples.

7 Conclusions

In the world of astrophysics, regression is both important and complicated by the nature of the types of data encountered. All approaches to regression can be seen as a way to compress the information contained in the data into just a few numbers such as the regression coefficients, predicted values or a measure of the support given by the data to a model. In this article we have attempted to review some of the modelling problems which arise and to summarise some of the techniques which have arisen to tackle them. We have also perhaps revealed a personal bias towards Bayesian approaches.

Astronomy is facing an exponential increase in the number and complexity of analyses. We are rapidly exhausting analyses not requiring complex (regression) models. The ease with which the Bayesian approach addresses the awkward features of the astronomical data makes it more and more appealing.

Acknowledgements

We are grateful to the anonymous referees and the Associate Editor for their helpful comments on an earlier version of this paper.

A Appendix

We stress that once the regression model is stated in mathematical terms such as in Equations (18) and (19), Bayesian tools such as BUGS [43] or JAGS [44] convert these equations into code and perform the necessary stochastic computations. Distribution of predicted values are also a standard output of these tools. Equations listed in the text find an almost literal translation in JAGS: Poisson, Normal, Uniform and Student t distributions become `dpois`, `dnorm`, `dunif`, `dt`, respectively. For some distributions, it is necessary to express them as particular cases of other distributions, for example the χ^2 is a particular form of the Gamma distribution. JAGS, following BUGS uses precisions, $prec = 1/\sigma^2$, in place of variances σ^2 . Furthermore, they use natural logarithms rather than decimal ones. The `<-` symbol reads “takes the value of”, the `~` symbol reads “is distributed as”. x^y is coded as `pow(x,y)` in JAGS.

A.1 Code for the Bayesian error-in-variable regression, Section 4.7

```
model
{
  for (i in 1:length(obsx))
  {
    x[i] ~ dunif(-1.0E+4,1.0E+4)
    obsx[i] ~ dnorm(x[i],prec.x[i])
    y[i] ~ dnorm(b+a*x[i], prec.scats)
    obsy[i] ~ dnorm(y[i],prec.y[i])
  }
  prec.scats ~ dgamma(1.0E-2,1.0E-2)
  b ~ dnorm(0.0,1.0E-4)
  a ~ dt(0,1,1)
}
```

A.2 Code for generating simulated data in Section 5.2

```
model
```

```

{
  x ~ dt(0.1,pow(1.1,-2),10)
  y <- 1.0 * x + 0.0
  obsx ~ dnorm(x,1)
  obsy ~ dnorm(y,1)
}

```

A.3 Code for Bayesian regression model in Section 5.2

```

model
{
  alpha ~ dnorm(0.0,1.0E-4)
  beta ~ dt(0,1,1)
  for (i in 1:length(obsx))
  {
    obsx[i] ~ dnorm(x[i],prec.obsx[i])
    obsy[i] ~ dnorm(y[i],prec.obsy[i])
    y[i] <- alpha+beta*x[i]
# t prior for the x population OR
  x[i] ~ dt(0.1,pow(1.1,-2),10)
# N(0,1) prior for the x population OR
  x[i] ~ dnorm(0,1)
# Normal prior for the x population with hyperparameters
  x[i] ~ dnorm(mu,prec)
  }
  mu ~ dnorm(0,1.0E-4)
  prec ~ dunif(0.0,10.0)
}

```

In order to predict \tilde{y} values, it suffices to list the x^{obs} values for which \tilde{y} is needed, entering a “NA” = “not available” code for the corresponding y^{obs} value to indicate to the program that they should be estimated.

A.4 Code for Bayesian regression model Equation (31) illustrated in Figure 2(a)

```

data
{
  nu <-6
}
model
{
  for (i in 1:length(obstot))
  {
    obsbkg[i] ~ dpois(nbkg[i])
    obstot[i] ~ dpois(nbkg[i]/C[i]+n200[i])
    n200[i] ~ dunif(0,3000)
    nbkg[i] ~ dunif(0,3000)
    precy[i] ~ dgamma(1.0E-5,1.0E-5)
    obslgM200[i] ~ dnorm(lgM200[i],precy[i])
    obsvarlgM200[i] ~ dgamma(0.5*nu,0.5*nu*precy[i])
    z[i] <- alpha+14.5+beta*(log(n200[i])/2.30258-1.5)
  }
  intrscat <- 1/sqrt(prec.intrscat)
  prec.intrscat ~ dgamma(1.0E-5,1.0E-5)
  alpha ~ dnorm(0.0,1.0E-4)
  beta ~ dt(0,1,1)
}

```

References

- [1] E. P. Hubble. Cepheids in spiral nebulae. *The Observatory*, 48:139–142, 1925.
- [2] D. C. Koo. Optical multicolors - A poor person's Z machine for galaxies. *Astronomical Journal*, 90:418–440, 1985.
- [3] S. Andreon and M.A. Hurn. The scaling relation between richness and mass of galaxy clusters: a Bayesian approach. *Monthly Notices of the Royal Astronomical Society*, 404(4):1922–1937, 2010.
- [4] A.R. Liddle. Information criteria for astrophysical model selection. *Monthly Notices of the Royal Astronomical Society: Letters*, 377(1):L74–L78, 2007.
- [5] R. Trotta. Bayes in the sky: Bayesian inference and model selection in cosmology. *Contemporary Physics*, 49(2):71–104, 2008.
- [6] T. Isobe, E.D. Feigelson, M.G. Akritas, and G.J. Babu. Linear regression in astronomy. *The astrophysical journal*, 364:104–113, 1990.
- [7] T.R. Lauer, S. Tremaine, D. Richstone, and S.M. Faber. Selection Bias in Observing the Cosmological Evolution of the M_{\bullet} - σ and M_{\bullet} -L Relationships. *The Astrophysical Journal*, 670:249, 2007.
- [8] W. Ubachs and E. Reinhold. Highly Accurate H₂ Lyman and Werner Band Laboratory Measurements and an Improved Constraint on a Cosmological Variation of the Proton-to-Electron Mass Ratio. *Physical Review Letters*, 92(10):101302, 2004.
- [9] M.G. Akritas and M.A. Bershadsky. Linear regression for astronomical data with measurement errors and intrinsic scatter. *The Astrophysical Journal*, 470:706, 1996.
- [10] J.P. Buonaccorsi. *Measurement error: models, methods, and applications*. Chapman & Hall/CRC, 2009.
- [11] S. Andreon and M.A. Hurn. X-ray scaling relations with non-ignorable selection function. In preparation.
- [12] F. Pacaud, M. Pierre, C. Adami, B. Altieri, S. Andreon, L. Chiappetti, A. Detal, P.A. Duc, G. Galaz, A. Gueguen, et al. The XMM-LSS survey: the Class 1 cluster sample over the initial 5 deg² and its cosmological modelling. *Monthly Notices of the Royal Astronomical Society*, 382(3):1289–1308, 2007.
- [13] S. Andreon and A. Moretti. Do X-ray dark, or underluminous, galaxy clusters exist? *Astronomy and Astrophysics*, 536(A37), 2011.
- [14] S.W. Allen, A.E. Evrard, and A.B. Mantz. Cosmological Parameters from Observations of Galaxy Clusters. *Annual Review of Astronomy and Astrophysics*, 49:409–470, 2011.
- [15] A.S. Eddington. On a formula for correcting statistics for the effects of a known error of observation. *Monthly Notices of the Royal Astronomical Society*, 73:359–360, 1913.
- [16] K.G. Malmquist. *Lund Medd. Ser. II*, 22:1–39, 1920.
- [17] A. Kenter, S.S. Murray, W.R. Forman, C. Jones, P. Green, C.S. Kochanek, A. Vikhlinin, D. Fabricant, G. Fazio, K. Brand, et al. XBootes: An X-Ray Survey of the NDWFS Bootes Field. II. The X-Ray Source Catalog. *The Astrophysical Journal Supplement Series*, 161:9, 2005.

- [18] S. Andreon. A Bayesian approach to galaxy evolution studies. *Bayesian Methods in Cosmology*, edited by Michael P. Hobson, Andrew H. Jaffe, Andrew R. Liddle, Pia Mukeherjee and David Parkinson. Published: Cambridge University Press, New York, Cambridge, UK; 2010, p. 265, page 265, 2010.
- [19] P. J. Humphrey, W. Liu, and D. A. Buote. χ^2 and Poissonian Data: Biases Even in the High-Count Regime and How to Avoid Them. *The Astrophysical Journal*, 693:822–829, 2009.
- [20] A.C. Atkinson. *Plots, transformations, and regression*. Clarendon Press Oxford, 1985.
- [21] S. Andreon, J.C. Cuillandre, E. Puddu, and Y. Mellier. New evidence for a linear colour–magnitude relation and a single Schechter function for red galaxies in a nearby cluster of galaxies down to $M^* + 8$. *Monthly Notices of the Royal Astronomical Society*, 372(1):60–68, 2006.
- [22] S. Andreon. The build-up of the red sequence in the galaxy cluster MS1054-0321 at $z = 0.831$. *Monthly Notices of the Royal Astronomical Society*, 369:969–975, 2006.
- [23] M. Hurn, A. Justel, and C.P. Robert. Estimating mixtures of regressions. *Journal of Computational and Graphical Statistics*, 12(1):55–79, 2003.
- [24] J. Gillard. An overview of linear structural models in errors in variables regression. *REVSTAT–Statistical Journal*, 8(1):57–80, 2010.
- [25] N.R. Draper and H. Smith. *Applied Regression Analysis (Wiley Series in Probability and Statistics)*. Wiley-Interscience, 1998.
- [26] W.H. Press, S.A. Teukolsky, W.T. Vetterling, and B.P. Flannery. *Numerical recipes*. Cambridge University Press, Cambridge, third edition, 2007.
- [27] B.C. Kelly. Some aspects of measurement error in linear regression of astronomical data. *The Astrophysical Journal*, 665:1489, 2007.
- [28] W. Cash. Parameter estimation in astronomy through application of the likelihood ratio. *The Astrophysical Journal*, 228:939–947, 1979.
- [29] R.J. Carroll, D. Ruppert, L.A. Stefanski, and C.M. Crainiceanu. *Measurement Error in Nonlinear Models: A Modern Perspective*. Chapman and Hall/CRC, second edition, 2006.
- [30] G. Casella and R.L. Berger. *Statistical Inference*. Duxbury, second edition, 2002.
- [31] R.J. Carroll and D. Ruppert. The use and misuse of orthogonal regression in linear errors-in-variables models. *American Statistician*, 50:1–6, 1996.
- [32] J. R. Gott, III, M. S. Vogeley, S. Podariu, and B. Ratra. Median statistics, h_0 , and the accelerating universe. *The Astrophysical Journal*, 549:1–17, 2001.
- [33] P.J. Huber and E.M. Ronchetti. *Robust statistics*. Wiley, second edition, 2009.
- [34] R.G.J. Miller. *Survival analysis*. Wiley, New York. US, 1981.
- [35] J. Schmitt. Statistical analysis of astronomical data containing upper bounds—General methods and examples drawn from X-ray astronomy. *The Astrophysical Journal*, 293:178–191, 1985.
- [36] T. Isobe, E.D. Feigelson, and P.I. Nelson. Statistical methods for astronomical data with upper limits. II—Correlation and regression. *The Astrophysical Journal*, 306:490–507, 1986.

- [37] E.D. Feigelson and P.I. Nelson. Statistical methods for astronomical data with upper limits. I- Univariate distributions. *The Astrophysical Journal*, 293:192–206, 1985.
- [38] A.P. Dempster, N.M. Laird, and D.B. Rubin. Maximum likelihood from incomplete data via the EM algorithm. *Journal of the Royal Statistical Society. Series B (Methodological)*, 39(1):1–38, 1977.
- [39] M. Lavalley, T. Isobe, and E. Feigelson. ASURV: Astronomy Survival Analysis Package. In *Astronomical data analysis software and systems I*, volume 25, page 245, 1992.
- [40] G. D’Agostini. Fits, and especially linear fits, with errors on both axes, extra variance of the data points and other complications. *Arxiv preprint physics/0511182*, 2005.
- [41] G. D’Agostini. *Bayesian reasoning in data analysis: A critical introduction*. World Scientific Pub Co Inc, 2003.
- [42] P. Dellaportas and D.A. Stephens. Bayesian analysis of errors-in-variables regression models. *Biometrics*, 51(3):1085–1095, 1995.
- [43] D. Lunn, D. Spiegelhalter, A. Thomas, and N. Best. The BUGS project: Evolution, critique and future directions. *Statistics in Medicine*, 28(25):3049–3067, 2009.
- [44] M. Plummer. *JAGS Version 2.2.0 user manual*, 2010.
- [45] A. Gelman. Prior distributions for variance parameters in hierarchical models. *Bayesian Analysis*, 1(3):515–533, 2006.
- [46] S. Andreon, R. de Propris, E. Puddu, L. Giordano, and H. Quintana. Scaling relations of the colour-detected cluster RzCS 052 at $z = 1.016$ and some other high-redshift clusters. *Monthly Notices of the Royal Astronomical Society*, 383:102–112, 2008.
- [47] S. Andreon and M. Huertas-Company. Red sequence determination of the redshift of the cluster of galaxies JKCS 041: $z \sim 2.2$. *Astronomy & Astrophysics*, 526:A11, 2011.
- [48] A. Gelman, J.B. Carlin, H.S. Stern, and D.B. Rubin. *Bayesian Data Analysis*. Champan and Hall/CRC, 2004.
- [49] S. Andreon and J. Bergé. Richness-mass relation self-calibration for galaxy clusters. *Astronomy and Astrophysics*, in press, 2012.
- [50] M. M. Phillips. The absolute magnitudes of Type IA supernovae. *The Astrophysical Journal Letters*, 413:L105–L108, 1993.
- [51] M. C. March, R. Trotta, P. Berkes, G. D. Starkman, and P. M. Vaudrevange. Improved constraints on cosmological parameters from Type Ia supernova data. *Monthly Notices of the Royal Astronomical Society*, 418:2308–2329, 2011.
- [52] A. Diaferio, L. Ostorero, and V. Cardone. Gamma-ray bursts as cosmological probes: Λ CDM vs. conformal gravity. *Journal of Cosmology and Astroparticle Physics*, 10:8, 2011.
- [53] S. Andreon. Understanding better (some) astronomical data using Bayesian methods. *Astrostatistical Challenges for the New Astronomy*, edited by J. Hilbe., Publisher: Springer Series on Astrostatistics, in press, 2012.
- [54] S. Perlmutter and B. P. Schmidt. Measuring Cosmology with Supernovae. In K. Weiler, editor, *Supernovae and Gamma-Ray Bursters*, volume 598 of *Lecture Notes in Physics*, Berlin Springer Verlag, pages 195–217, 2003.

[55] S. Andreon. The enrichment history of the intracluster medium: a Bayesian approach. *Astronomy and Astrophysics*, 546:A6, 2012.

To be put as footnote to "references" Most of the mentioned papers are freely available from ADS, <http://adsabs.harvard.edu/index.html>, clicking the X or G links.